Computational design of Checkpoint Kinase-1 (CHK-1) inhibitors for cancer therapy

Jaikanth Chandrasekaran
Sri Ramachandra Institute of Higher education and Research (Deemed to be University
Saptami Kanekar
Yenepoya (Deemed to be University)
Shobha Dagamajalu
Yenepoya (Deemed to be University)
Prashanth Modi
Yenepoya (Deemed to be University)
Kirthika Gopinathan
Sri Ramachandra Institute of Higher education and Research (Deemed to be University
Rajesh Raju
Yenepoya (Deemed to be University)
T. S. Keshav Prasad
Yenepoya (Deemed to be University)
Rex Devasahayam Arokia Balaya (rexprem@yenepoya.edu.in)
Yenepoya (Deemed to be University)

Research Article

Keywords: Cancer therapy, Repurposing, Check Point Kinase-1 (CHK-1) Inhibitor, Procaterol, e-pharmacophore modelling, Prime MM-GBSA, ADME-Toxicity prediction & MD simulations

Posted Date: January 3rd, 2023

DOI: https://doi.org/10.21203/rs.3.rs-2414645/v1

Abstract

CHK-1 kinase belongs to the serine/threonine family of kinases, which play a vital role in cell cycle arrest and proved to be a promising therapeutic target to control cancer development and progression. Many potent and selective CHK-1 inhibitors have been reported, but only a few are currently in clinical trial. In this era, drug re-profiling has proved to be a major step in drug discovery and development that is cost and time beneficial. In this study, we have incorporated a combined *in silico* computational approach to widen the chemical range of CHK-1 inhibitors from the existing FDA approved drugs. An e-pharmacophore model was created from 3D crystal coordinates of CHK-1 protein complex with the clinical trial inhibitor (CCT245737). The hypothesis with seven molecular features was screened with FDA drugs and the obtained drugs were subjected into Glide XP molecular docking. The top 10% scored ligands were visualized and Procaterol was best identified which showed similar interaction patterns with enzyme active sites as the clinical trial inhibitor. Furthermore, total binding free energy, pharmacokinetic properties and molecular dynamics were also evaluated. The results consolidated showed better binding affinity, acceptable kinetic profile and significant stability of Procaterol binding with CHK-1 kinase. In conclusion, we highlight that Procaterol is a re-provable potent CHK-1 inhibitor and appears as a new structural scaffold for further optimisation.

Introduction

Cancer is one among the world's most deadly diseases, causing millions of people die every year. A vast range of proteins have been linked to tumour formation and progression (1–3), with kinases (4) being the most intriguing. Tyrosine kinase inhibitors, namely the epidermal growth factor receptor (EGFR), are being positioned as drugs (5), bringing attention to serine-threonine kinases, which play a critical role in carcinogenesis (6). These kinases catalyse the phosphorylation of serine/threonine residues on the substrate protein. Checkpoint kinase 1 (Chk1) (7), Pim-1 Proto-Oncogene, Serine/Threonine Kinase (PIM1) (8), MAPK/extracellular signal-regulated kinase (MEK1) (9), and Cyclin-dependent kinases (CDKs) (10) have all recently been identified as promising targets for the development of cancer progression inhibitors.

Cell cycle check points serve as a barrier between each phase of the cell cycle, allowing the entire process to be slowed or paused in order to ensure precise duplication and transmission of genetic material to progeny cells, or to enable time for DNA repair. In response to DNA damage, Chk 1 (ChK1) initiates the phosphorylation of both ATR (Ataxia-telengiectasia and Rad3-related) and ATM (Ataxia-telengiectasia, mutant), accompanied by phosphorylation of a range of substrates and the start of signal cascades which culminate in cell-cycle arrest (11). The checkpoint effectors (CDC25A and CDC25C, p53, and BRCA1) are phosphorylated/activated when ATM and ATR are activated. This is accomplished by phosphorylation/activation of the Chk1 and Chk2 kinases (12).

The Chk1 is an important kinase that plays a key role in cell cycle arrest. The DNA damage sensor and cell death pathway stimulator Checkpoint kinase 1 (*CHEK1*) is considered an oncogene in tumours, where its actions are crucial for tumorigenesis and the survival of cancer cells treated with chemotherapy and radiotherapy (13). Given the growing importance of Chk1 inhibitors in cancer treatment, there is a demand for a wider chemical range of Chk1 inhibitors.

Hence, the distinguishable role of Chk-1 and Chk-2 in DNA repair mechanism of normal and tumour cells, exposes CHK-1 as a master regulator and making it a viable emerging biological target for therapeutic intervention. Unfortunately, there are few clinical trial candidates in the early phases of clinical trial (14). However, the barriers in novel drug development such as prolonged time, large capital and effort make us look for alternative strategies (15). Drug reprofiling is one such strategy to explore novel uses for approved drugs.

Based on this collective insight, we implicated *in-silico* repurposing strategies, comprising of e-Pharmacophore modelling, molecular docking, molecular dynamics, molecular mechanics and ADME prediction to identify an effective Chk-1 selective inhibitor for a better and efficient treatment regimen.

Materials And Methods

Protein preparation and its structure validation

The co-crystallized 3D structure of CHK-1 protein complexed with clinical trial inhibitor (CCT245737) was obtained from PDB (ID: 5F4N) and subjected to protein preparation using “Protein preparation Wizard” of Schrodinger suite (Schrödinger, LLC, New York, NY, 2019-

\1). In the protein pre-process step, the bond orders were aligned, followed by proper coordinates fixing for missing side chains and loops using PRIME and addition of missing hydrogen atoms. All water molecules below 5Å from co-crystallized ligand were kept to ensure the presence of water for protein-ligand binding interactions. Finally, the energy minimization was carried out using OPLS3e force field. The above pre-processed and minimized structure of CHK-1 protein was validated by the inspection of phi/psi distribution of Ramachandran Plot obtained through PROCHEK analysis. Additionally, the CHK-2 protein (PDB:2CN8) was also prepared, minimized and validated similar as that of CHK-1 for selectivity evaluation purpose.

Receptor grid generation

Once the protein preparation was completed, the receptor grid was generated using OPLS-3e force field by “Receptor Grid Generation” panel in Schrodinger suite (Schrödinger, LLC, New York, NY, 2019-1). Both internal and external grid boxes were generated by selecting the hit atoms of co-crystallized ligand to specify the ATP binding pocket of inhibitors. This process facilitates the exclusion of co-crystallized ligand from protein binding site and favours the molecular docking of ligand library.

E-pharmacophore hypothesis generation

In this study, the PHASE v3.8 module of Schrodinger suite (Schrödinger, LLC, New York, NY, 2020-2) was utilized to build an e-pharmacophore model. The respective features for database screening were selected from the better re-docked pose of co-crystallized ligand (CCT245737) after analysing the XP- Visualizer information of reward and penalty regions (16). Briefly, phase module provided a set of six features such as Hydrogen bond acceptors (A), Hydrogen bond donors (D), Hydrophobic groups (H), Negatively ionisable groups (N), Positively ionisable groups (P) and Aromatic rings (A). Based on the existing knowledge of CHK-1 protein-ligand interaction and the XP-visualizer description, we manually selected essential chemical features for further database screening.

Ligand preparation

All the approved FDA drug candidates were retrieved as 2D structure data file (SDF) from “Drugbank” database and incorporated into ligand preparation using “LigPrep” software package of GLIDE V7.7 (Schrödinger, LLC, New York, NY, 2019-1). This structural refinement process was performed with following parameters: (a) force field OPLS-3e for energy minimization, (b) ionization state generation at the pH of 7.0 ± 2.0, (c) appropriate tautomer generation using Epik v4.0, (d) desalt option activation to neutralize the structure and, (e) chirality information retainment by setting to generate 32 isomers per ligand. The conformers generated from the above ligand preparation process were incorporated into database creation using “Create Phase Database” panel of PHASE v3.8 module of Schrodinger suite. The ligands were filtered based on Qikprop properties, Lipinski’s rule and reactive functional groups during database creation.

Pharmacophore based virtual screening

Virtual database screening of e-pharmacophore was employed to separate the pharmacophore matched drug candidates from the FDA drug database by utilizing the PHASE v3.8 module Schrodinger suite (Schrödinger, LLC, New York, NY, 2019-1). This database screening enables ligands that show similar chemical features as that of co-crystallized clinical trial ligand. The pharmacophore matched ligands after screening were ranked in order of the fitness score ranging from 0 to 3, as applied in the PHASE.

Molecular docking

Prior to molecular docking, the accuracy of the docking program was validated based on the calculation of root mean square deviation (RMSD) value. Firstly, the co-crystallized ligand was extracted from the binding pocket and re-docked with same protein. Then, the re-docked ligand conformation was superimposed with original native ligand conformation and the RMSD value was calculated. The calculated RMSD value less than 1 confirmed the accuracy of docking program.

e-pharmacophore matched FDA drug candidates obtained from the database screening was subjected to molecular docking protocol using GLIDE V7.7 of Schrodinger suite (Schrödinger, LLC, New York, NY, 2019-1). The compounds were flexibly docked with the ATP binding pocket of CHK-1 protein using Extra Precision (XP) scoring function to estimate the protein-ligand binding affinity. For the top 10% docked ligands, the docking score, G score and nature of protein interactions were examined manually using MAESTRO version (Schrodinger) and the best drug candidates were scrutinized for further computational analysis.

QikProp ADME/Toxicity properties prediction

Experimentally more relevant pharmacokinetic and toxicity properties of selected drug candidates were predicted computationally using a precise software package of QikProp v5.4 incorporated in the Schrodinger suite (Maestro11.9.011, Schrödinger, LLC, New York, NY, 2019-1). Further, it also facilitated the estimation of drug-like characteristics through application of Lipinski's rule-of-five and Jorgensen's rule-of-three infringements.

Molecular Mechanics –Generalized Born Surface Area (MM-GBSA) calculation

The effect of solvent on ligands' binding free energies (ΔG bind) was estimated with Prime MM-GBSA tool of PRIME v3.5 module incorporated Schrodinger suite (Schrödinger, LLC, New York, NY, 2019-1). Briefly, the Glide XP docked poses of both co-crystallized clinical trial inhibitor and scrutinized FDA drug candidates were minimized and the total free binding energies were computed by implementing the VSGB as a solvent model, OPLS-3e as a force field and having remaining parameters unchanged. Theoretically, the binding free energies were calculated based on the following equation:

$$\Delta G\ bind = \Delta E_{MM} + \Delta G_{Solv} + \Delta G_{SA}$$

where, ΔE_{MM} is the difference between the minimized energies of CHK-1 protein-Inhibitor complex and sum of minimized unbound CHK-1 protein and its inhibitor, ΔG_{Solv} is the difference between the GBSA solvation energies of CHK-1 protein- inhibitor complex and sum of GBSA solvation

energies of unbound CHK-1 protein and its inhibitor, and ΔG_{SA} is the difference between the surface area energies of CHK-1 protein- inhibitor complex and sum of surface area of unbound protein and its inhibitor.

Molecular Dynamics

MD simulations are advanced computational tools that can be utilized effectively to analyse the stability, RMSD and interaction of selected ligands in a flexible macromolecular environment using DESMOND V5.2 module of Schrodinger suite (Schrödinger, LLC, New York, NY, 2020-2). During simulation, the atoms of protein-ligand complex were allowed to interact for a brief period of 200 ns and the physical movements of complex were evaluated at atomistic level. Firstly, the docked protein-ligand complex was incorporated in orthorhombic simulation box solvated with TIP3P (transferable intermolecular potential with 3 points) explicit water model. The simulation system was again recalculated to neutralize the overall charge by adding suitable counterions in the system builder panel. Additionally, 0.15 M NaCl salt concentrations were fixed, 20 Å away from the ligand to simulate background isosmotic salt environment. The above prepared system was incorporated in workspace and subjected to run MD simulation using NPT ensemble at 300K temperature and 1.01325 bars atmospheric pressure with the assistance of OPLS_3e molecular mechanic's force field. During 200 ns of simulation time, the structure frames were recorded in the trajectory at every 100ps and a total of 2000 frames were saved. Finally, the simulation interaction diagram tool of DESMOND V5.2 was used to sketch the MD simulation results.

Results And Discusssion

Human CHK-1 is a nuclear protein and it consists of a highly conserved N-terminal kinase domain and less conserved C-terminal region (17). The X-ray crystallographic solid foundation of human CHK-1 kinase protein and its complex with ATP (an endogenous agonist) and other clinical trial inhibitors (UCN-01, CCT245737, Rabuseritib, Prexasertib, GDC-0575) briefly delineates the five essential regions namely, (a) the hinge region, (b) the ribose binding pocket, (c) the solvent exposed region, (d) the water pocket and (e) the polar (18, 19). The highly conserved hinge region containing Cys-87 and Glu-85 amino acids and the ligand binding to this region potentiates the inhibitory activity. The major amino acid residues such as Tyr-20, Lys-38, Glu-55, Asn-59, Phe-149 and Ser-147 that are present in the interior water pocket and polar region are unique for CHK-1 kinase and is occupied by three water molecules. The binding interaction of ligand functional groups in this region increases the CHK-1 kinase selectivity. There is also a ribose binding pocket that consists of hydrophilic amino acids like Glu-91, Glu-134 and Asn-135. Similarly, the exposed region is situated only a few amino acid residues away from the hinge region The presence of polar and highly electronegative groups increases the ligand stability and kinase inhibitory (18, 20). (Fig. 1a).

e-Pharmacophore Modelling

Pharmacophore modelling is a 3D special arrangement of molecular features to recognize the suitable ligands for selected biological macromolecules (21). Compared to the traditional pharmacophore modelling, e-pharmacophore hypothesis incorporates both stereo-electronic features of the ligand with the energetics of its interactions with the protein structure (22). It serves as a powerful filter tool for virtual screening and utilizes the Glide XP scoring function to characterise the protein-ligand interactions.

The present study generated an e-pharmacophore hypothesis from 3D crystal coordinates of CHK-1 protein complex with a potent and selective clinical trial inhibitor (CCT245737). Initially the protein structure was obtained from Protein Data Bank (PDB ID: 5F4N; Resolution: 1.91Å) and was prepared using protein preparation wizard. Subsequently, the prepared protein structure was validated through Ramachandran plot by visualizing the stereo-chemical spatial arrangement of the amino acid residues. From the above protein structure, the native ligand was extracted and re-docked with same binding pocket using Glide XP docking mode. The binding of the re-docked co-crystalized ligand in the ATP binding site was visualized with the help of XP-Visualizer application and simultaneously the reward and penalty regions were estimated.

The protein-ligand interactions of CHK-1 with CCT245737 ligand included (a) the two H-bond interactions in the hinge region involving the backbone NH-group of Cys-87 and backbone carbonyl group of Glu-85 amino acid residues; (b) H-bond and salt bridge interactions formed with the sidechain carbonyl group and acidic residue of Glu-91 amino acid residue, in the ribose binding pocket and (c) occupation of highly electronegative halogen group (Fluorine) in solvent exposed region which increases the protein-ligand stability (Fig. 1b **& c**).

Based on the insight of XP-visualizer information and protein -ligand interaction, we developed an e-pharmacophore hypothesis with seven essential molecular features AADPRRR (Two- Hydrogen bond acceptors (A), One- Hydrogen bond donor (D), One-Positively ionisable group (P) and Three- Aromatic rings (R)) to retrieve the reprovable FDA approved drug candidate from further database screening. The generated e-phamacophoric features were illustrated in Fig. 2.

e-pharmacophore hypothesis screening and molecular docking

The pharmacophore features were incorporated in PHASE module and allowed for previously prepared database screening. To retrieve a more promising FDA drug for CHK1 inhibition, we fixed 4 minimum matching criteria from the generated 7 pharmacophore features. After database screening we obtained 812 drug candidates with maximum fitness score of 1.867 and used for further molecular docking studies.

Recently, numerous studies have used molecular docking method to identify the suitable drug molecule for the target of interest (23). It is carried out to exclude those inactive drug candidates from the above e-pharmacophore based screening to obtain most favourable compounds. In our study, the RMSD value of re-docked clinical trial ligand (CCT245737) was substantially low (0.4387), and conformed the accuracy of docking program to screen and predict the binding affinity of above obtained 812 ligands with CHK-1 protein (**Supplementary Fig.S1**). Finally, the Extra precision (XP) molecular docking program was opted for above obtained FDA drugs, and 167 drugs were docked into the ATP binding site of CHK-1 protein. The molecular docking produced ligand docking score, Glide score along with bond interaction distance values (24). The binding modes of all 167 drug candidates were ranked based on the docking score and the top 10% ligands were visually analysed for nature of protein-ligand interactions and binding affinity (Table 1). Interaction fingerprints depends on both specific interactions at the binding site and the non-specific force outside the target binding pocket. The binding mode structures of top 10% ligands are illustrated in **supplementary Fig.S2**.

Table 1
Extra precision docking results of top 10% FDA compounds obtained through e-pharmacophore screening approach.

Drug name	Docking score	Glide G Score	Interaction Residue	Nature of Interactions	Fitness score
Methotrimeprazine	-10.505	-10.505	Glu-91	H-bond (1.70Å)	1.750
				Salt bridge (4.82 Å)	
Acepromazine	-10.358	-10.385	Glu-91	H-bond (1.68Å)	1.738
				Salt bridge (4.84 Å)	
Promazine	-9.721	-9.721	Glu-91	H-bond (1.67Å)	1.757
				Salt bridge (4.79 Å)	
Procaterol	-9.466	-9.734	Glu-85	H-bond (2.47Å)	1.568
			Glu-91	H-bond (1.83Å)	
			Cys-87	H-bond (1.92Å)	
				Salt bridge (4.84 Å)	
Carvedilol	-9.297	-9.406	Glu-85	H-bond (1.90Å)	1.569
			Glu-91	H-bond (1.82Å)	
				H-bond (2.15Å)	
				Salt bridge (4.94 Å)	
Alimemazine	-9.289	-9.289	Glu-91	H-bond (1.73Å)	1.762
				Salt bridge (4.83 Å)	
Ropinirole	-9.026	-9.026	Glu-85	H-bond (1.63Å)	1.621
			Cys-87	H-bond (2.05Å)	
Methodilazine	-9.011	-9.011	Glu-91	H-bond (1.91 Å)	1.797
				Salt bridge (4.87 Å)	
Propiomazine	-8.913	-8.913	Glu-91	H-bond (1.82 Å)	1.648
Aceprometazine	-8.873	-8.873	-	-	1.660
Mesoridazine	-8.738	-8.873	Glu-91	H-bond (1.64 Å)	1.842
				Salt bridge (4.74Å)	
Dexrazoxane	-8.586	-9.041	Glu-85	H-bond (1.88Å)	1.522
			Cys-87	Salt bridge (4.84Å)	
			Glu-91	H-bond (1.99Å)	
Encainide	-8.489	-8.489	Cys-87	H-bond (2.07Å)	1.677
Promethazine	-8.408	-8.408	Glu-91	H-bond (2.33Å)	1.701
Cyamemazine	-8.231	-8.231	Glu-91	H-bond (1.82 Å)	1.723
				Salt bridge (4.95Å)	
Isothipendyl	-8.191	-8.191	-	-	1.694
CCT245737	-10.190	-11.468	Glu-85	H-bond (2.13Å)	-
			Cys-87	H-bond (2.22Å)	
			Glu-91	H-bond (1.48Å)	
				Salt bridge (4.56Å)	

From the top 10% scored ligands, we noticed that the Procaterol and Dexrazoxane drugs possess better binding affinity as well as important key interactions with the ATP binding pocket of CHK-1 protein. More elaborately, Procaterol showed double hydrogen bond interactions with hinge region amino acid residue Glu-85 as well as single hydrogen bond interaction with Glu-91 and Cys 87 residues present in the ribose pocket and

hinge region respectively (Fig. 3a **& b**). Similarly, Dexrazoxane forms hydrogen bond with Glu-85 and Cys-87 amino acid residues of hinge region and Glu-91 residue of Ribose binding pocket (Fig. 3c **& d**). We selected Procaterol and Dexrazoxane for further computational analysis based on the knowledge of existing CHK-1 inhibitors and binding site requirements.

Further, we elucidated the selectivity and potency of Procaterol and Dexrazoxane with CHK-2 protein by molecular docking using Glide XP scoring function. The 3D crystal structure of human CHK-2 protein complex with potent inhibitor (Debromohymenialdisine) with 2.70Å resolution was obtained from "Protein Data Bank" and structural refinement was performed using Protein Preparation Wizard. Similar to that of CHK-1 protein, the RMSD value of superimposition was found to be low (0.674) and it delineated the accuracy of docking (**Supplementary Fig.S3**).

After validation of the docking program, both clinical trial ligand (CCT245737) and the two selected FDA drugs were docked with ATP binding pocket of CHK-2 protein using Glide Extra Precision mode. The docking score of CCT245737, Procaterol and Dexrazoxane was found to be -6.369, -3.497 and − 5.489 kcal/mol respectively (**Supplementary Fig.S4**). This molecular docking shows that procaterol and dexrazoxane possess less binding affinity towards CHK-2 than the clinical trial ligand.

In silico **prediction of Pharmacokinetic (ADME) and toxicity parameters using Qikprop**

Generally, the Qikprop module analyses and calculates physiologically suitable pharmacokinetic and toxicity parameters and provides information about the safety range for all selected drug molecules (25). In this study we performed Qikprop screening for the already existing FDA approved drugs - Procaterol and Dexrazoxaneto compare their pharmacokinetic and toxicity parameters with the clinical trial inhibitor. The results of Qikprop data are shown in Table 2. All selected drug candidates show the acceptable range of drug likeness characteristics.

Table 2
The Selected drug candidates with their physicochemical and toxicity descriptors determined by Qikprop tool.

Compound Name[a]	Molecular weight (g/mol)[b]	QPlog$_{o/w}$[c]	QPlogS[d]	QPlog HERG[e]	QPlogBB[f]	QP Caco[g]	#metab ± [h]	QPlogKhsa[i]	%human Oral Absorption[j]	RO5[k]	RO3[l]
CCT245737	379.34	0.985	-4.046	-5.639	-0.775	57.546	6	-0.385	64.22	0	0
Procaterol	290.36	0.805	-2.065	-4.839	-0.878	69.689	3	-0.301	64.67	0	0
Dexrazoxane	268.27	-2.328	0.023	-4.355	-0.822	2.538	6	-0.869	20.55	0	1

[a] Ligand name ; [b] Molecular weight of the compound (acceptable range: 130–725 g/ mol); [c] Predicted octanol/water partition co-efficient logP (acceptable range:-2.0 to 6.5) [d] Predicted aqueous solubility ; S in Mol/L (acceptable range:-6.5 to 0.5); [e] Predicted IC50 value for Blockage of HERG K^+ Channels (acceptable range: below − 5.0); [f] Predicted Blood Brain Barrier(BBB) permeability (acceptable range:-3.0 to 1.2); [g] Predicted apparent Caco-2 cell permeability in nm/sec (range: <25 poor, > 500 great) [h] Number of likely metabolic reactions (range: 1to 8);[l] Predicted Human serum albumin binding (acceptable range: -1.5 to 1.5);[j] Percentage of human oral absorption (< 25% is poor &>80% is high); [k]Number of violations in Lipinski rule of Five; [l] Number of violations of Jorgensen's rule of three.

Prime MMGBSA calculation

The Prime MMGBSA simulation tool can be utilized to predict the ligand binding energies and strain energies (26) of the selected drug candidates from previous computational steps. The low energy binding poses of CCT245737, Procaterol and Dexrazoxane with CHK-1 protein (5F4N) retrieved from Glide XP docking, were rescored based on the theoretical calculation of total binding free energies. Our results revealed the MMGBSA ΔG Bind score of CCT245737, Procaterol and Dexrazoxane to be -50.28, -48.35 and − 32.40 respectively. Interestingly, Procaterol displayed a better ΔG Bind score near the clinical trial inhibitor (CCT245737) than the Dexrazoxane molecule. Collectively MM-GBSA analysis suggested that Procaterol forms a more stable complex and possessed selective inhibition of CHK-1 protein like clinical trial inhibitor.

Molecular dynamics insight on protein-ligand stability

Molecular dynamics assign velocities and calculate forces on all atoms to provide an insight into dynamic perturbations within the protein-ligand complex and interactions of ligand with water molecules (27). It is carried out to understand the stability and conformational changes of ligand–protein complexes (28). Based on the results of Molecular docking, ADME/T prediction and MMGBSA analysis, Procaterol possesses better binding affinity, acceptable range of kinetic profile and lowest ΔG Bind score than Dexrazoxane. The protein-ligand stability of the above shortlisted Procaterol-CHK-1 complex was evaluated using Desmond MD simulation analysis and the results were compared with the reference inhibitor (CCT245737).

The MD results of clinical trial inhibitor (CCT245737)-CHK-1 complex is illustrated in Fig. 4. The dynamics trajectory events remained stable throughout the simulation process. Additionally, the stability of the complex was determined by plotting the RMSD graph during simulation. The Fig. 4a depicts the stability of CCT245737 CHK-1 complex and the PL-RMSD was found between the ranges of 0.50 to 3.2 Å. Subsequently, CHK-1

protein residues present in the hinge region, ribose binding pocket and polar region interacted with the ligand atoms and the complex was stabilized by different intermolecular interactions. Briefly, interaction patterns showed that 98% and 97% of H-bond interactions was formed with Glu-85 and Cys-87 in hinge region. Similarly, 95% of H-bond interactions was formed with Glu-91 residue present in ribose binding pocket. Also, it occupied the water pocket and forms Water Bridge (95% and 83%) and H-bond (39%) interactions with polar region residues Glu-55, Asn-59 and Asp-148 respectively.

The result obtained from the Procaterol-CHK-1 complex MD simulation and the results are showed in Fig. 5. The RMSD for the Procaterol-CHK-1 complex remained stable for 200 ns time frame with the Protein RMSD 2.25 Å and ligand RMSD within 0.25 to 4Å till the end of the simulation. Further, we examined the site at which Procaterol bound to the CHK-1 protein and found that it robustly interacted with CHK-1 residues present in the hinge region, ribose binding pocket and polar region. In short, the key interactions included, the 87% H- bond interaction as well as 71% were formed with hinge region residues Glu-85 and Cys-87 respectively. Similarly, 85% and 52% of water bridge interactions were formed in the polar and ribose binding pockets of Glu-91 amino acid residues. The results of XP-docking and Post-MD based intermolecular interactions for CHK1 protein with CCT245737 and Procaterol are summarised in Table 3. The overall MD results insisted that Procaterol is a preferable CHK-1 inhibitor since it has all the essential interactions as compared to the clinical trial inhibitor (CCT245737).

Table 3
The XP-docking and Post-MD based intermolecular interactions between protein-ligand complexes

	XP-docking based intermolecular interactions		**Post MD based intermolecular interactions (100ns, 200ns)**	
Drug Name	**Interaction Residue**	**Nature of interaction**	**Interaction Residue**	**Nature of major interaction factions**
CCT245737	Glu-85	H-bond	Glu-85	H-bond
	Glu-91	H-bond	Cys-87	H-bond
	Cys-87	H-bond	Glu-91	H-bond
		Salt bridge	Glu- 55	Water bridge
			Asn- 59	Water bridge
Procaterol	Glu-85	H-bond	Glu-85	H-bond
	Glu-91	H-bond	Cys-87	Water bridge
	Cys-87	H-bond	Glu-91	H-bond
		Salt bridge	Lys-38	H-bond
				Water bridge
				Water bridge

Conclusion

CHK-1 kinase is an ideal drug target for sensitizing cytotoxic agents and radiation therapeutics in many solid tumours. Therefore, the CADD technology is fundamental for novel and persuasive drug discovery studies. In this study, an integrated e-pharmacophore based virtual screening, XP molecular docking, Prime MM-GBSA, ADMET and molecular dynamics simulation has been successfully implemented to find re-purposable FDA drug candidates as CHK-1 inhibitors. Moreover, our virtual screening workflow clearly indicates that, Procaterol a long acting β2-receptor agonist shows better binding affinity, acceptable range of kinetic profile, lowest binding free energy and significant complex stability with ATP binding region of CHK-1 protein as like the clinical trial inhibitor (CCT245737). It also shares the lowest binding affinity with regard to active site of CHK-2 protein. Additionally, a significant interaction with essential regions of ATP binding site was viewed in both molecular docking and dynamics studies. The insight from this *in silico* approach would be very generous in pharmacologic lead discovery for CHK-1 kinase and amicably implicated in cancer treatment. Thus, we can spot out the structurally diverse FDA approved drug, Procaterol, which can be used as a scaffold to discover the potent and selective lead CHK-1 inhibitors.

Declarations

ACKNOWLEDGEMENTS

Authors thank Dr. M Vijaykumar, Vice Chancellor, *Yenepoya (Deemed to be University) and Dr. Jalaluddin Akbar.K.C, Additional professor, Yenepoya medical college for the project support. We also thank Yenepoya (Deemed to be University)* for providing the infrastructure facility for Centre for Integrative Omics Data Science. We also thank PSGCP *and MS Ramaiah University* for schrodinger and simulation support respectively.

Funding: This work was supported by Faizal and Shabana Foundation.

Conflict of interest : Authors declare no competing interest in any form.

Data availability : The data that support the findings of this study are available in the Supporting Information Material of this paper.

Author information

Authors and Affiliations

Sri Ramachandra Faculty of Pharmacy, Sri Ramachandra Institute of Higher education and Research (Deemed to be University) Porur, Chennai, India

Jaikanth Chandrasekaran, Kirthika Gopinathan

Centre for Integrative Omics Data Science, Yenepoya (Deemed to be University), Mangalore, Karnataka, India

Rex Devasahayam Arokia Balaya, Saptami Kanekar, Rajesh Raju

Center for Systems Biology and Molecular Medicine, Yenepoya Research Centre, Yenepoya (Deemed to be University), Mangalore, Karnataka, India

Shobha Dagamajalu, *Prashanth Modi, T. S. Keshava Prasad*

Corresponding author :

Correspondence to *Rex Devasahayam Arokia Balaya*

Author Contributions

Jaikanth Chandrasekaran*: Conceptualization, Investigation, Methodology, Visualization, Writing manuscript.* ***Saptami Kanekar****: Drafting, Reviewing and editing.* **Shobha Dagamajalu***: Reviweing and editing.* ***Prashanth Modi****: Reviweing and editing.* ***Kirthika Gopinathan****: Data analysis.* ***Rajesh Raju****: Reviweing and editing.* ***T. S. Keshava Prasad****: Reviweing and editing.* ***Rex Devasahayam Arokia Balaya****: Conceptualization, Project administration, Supervision, Visualization, Writing manuscript*

References

1. Choudhari R, Minero VG, Menotti M, Pulito R, Brakebusch C, Compagno M, et al. Redundant and nonredundant roles for Cdc42 and Rac1 in lymphomas developed in NPM-ALK transgenic mice. Blood. 2016;127(10):1297–306.
2. Galluzzi L, Kepp O, Vander Heiden MG, Kroemer G. Metabolic targets for cancer therapy. Nat Rev Drug Discov. 2013;12(11):829–46.
3. Hallberg B, Palmer RH. Mechanistic insight into ALK receptor tyrosine kinase in human cancer biology. Nat Rev Cancer. 2013;13(10):685–700.
4. Fabbro D, García-Echeverría C. Targeting protein kinases in cancer therapy. Curr Opin Drug Discov Devel. 2002;5(5):701–12.
5. Hartmann JT, Haap M, Kopp HG, Lipp HP. Tyrosine kinase inhibitors - a review on pharmacology, metabolism and side effects. Curr Drug Metab. 2009;10(5):470–81.
6. Capra M, Nuciforo PG, Confalonieri S, Quarto M, Bianchi M, Nebuloni M, et al. Frequent alterations in the expression of serine/threonine kinases in human cancers. Cancer Res. 2006;66(16):8147–54.
7. Tao ZF, Lin NH. Chk1 inhibitors for novel cancer treatment. Anticancer Agents Med Chem. 2006;6(4):377–88.
8. Merkel AL, Meggers E, Ocker M. PIM1 kinase as a target for cancer therapy. Expert Opin Investig Drugs. 2012;21(4):425–36.
9. Chang-Yew Leow C, Gerondakis S, Spencer A. MEK inhibitors as a chemotherapeutic intervention in multiple myeloma. Blood Cancer J. 2013;3(3):e105.
10. Malumbres M, Barbacid M. Cell cycle, CDKs and cancer: a changing paradigm. Nat Rev Cancer. 2009;9(3):153–66.
11. Qiu Z, Oleinick NL, Zhang J. ATR/CHK1 inhibitors and cancer therapy. Radiotherapy and Oncology. 2018;126(3):450–64.
12. Gao X, Han L, Ren Y. In Silico Exploration of 1,7-Diazacarbazole Analogs as Checkpoint Kinase 1 Inhibitors by Using 3D QSAR, Molecular Docking Study, and Molecular Dynamics Simulations. Molecules. 2016;21(5):591.
13. Ebili HO, Iyawe VO, Adeleke KR, Salami BA, Banjo AA, Nolan C, et al. Checkpoint Kinase 1 Expression Predicts Poor Prognosis in Nigerian Breast Cancer Patients. Molecular Diagnosis & Therapy. 2018;22(1):79–90.
14. Walton, M. I. *et al.* The clinical development candidate CCT245737 is an orally active CHK1 inhibitor with preclinical activity in RAS mutant NSCLC and Eμ-MYC driven B-cell lymphoma. Oncotarget (2016) doi:10.18632/oncotarget.4919.
15. Dugger, S. A., Platt, A. & Goldstein, D. B. Drug development in the era of precision medicine. Nature Reviews Drug Discovery (2018) doi:10.1038/nrd.2017.226.

16. Manual, U. Schrödinger Release 2019-3: Glide, Schrödinger, LLC, New York, NY, 2019. *Schrödinger Release 2018-3 LigPrep, Schrödinger, LLC, New York, NY, 2018.* (2018).
17. Kim, K. S., Choi, K. J. & Bae, S. A novel Chk1-binding peptide that enhances genotoxic sensitivity through the cellular redistribution of nuclear Chk1. Int. J. Mol. Med. (2016) doi:10.3892/ijmm.2016.2762.
18. Chen, X. M. *et al.* Structure-based and shape-complemented pharmacophore modeling for the discovery of novel checkpoint kinase 1 inhibitors. J. Mol. Model. (2010) doi:10.1007/s00894-009-0630-y.
19. Matthews, T. P., Jones, A. M. & Collins, I. Structure-based design, discovery and development of checkpoint kinase inhibitors as potential anticancer therapies. Expert Opinion on Drug Discovery (2013) doi:10.1517/17460441.2013.788496.
20. Reader, J. C. *et al.* Structure-guided evolution of potent and selective CHK1 inhibitors through scaffold morphing. J. Med. Chem. (2011) doi:10.1021/jm2007326.
21. Patel, P. *et al.* Pharmacophore Based 3D-QSAR, Virtual Screening and Docking Studies on Novel Series of HDAC Inhibitors with Thiophen Linker as Anticancer Agents. Comb. Chem. High Throughput Screen. (2016) doi:10.2174/1386207319666160801154415.
22. Arun, K. G., Sharanya, C. S., Abhithaj, J., Francis, D. & Sadasivan, C. Drug repurposing against SARS-CoV-2 using E-pharmacophore based virtual screening, molecular docking and molecular dynamics with main protease as the target. J. Biomol. Struct. Dyn. (2020) doi:10.1080/07391102.2020.1779819.
23. Luo, X. *et al.* Discovery of new small-molecule cyclin-dependent kinase 6 inhibitors through computational approaches. Mol. Divers. (2020) doi:10.1007/s11030-020-10120-3.
24. Ranjan, A., Chauhan, A. & Jindal, T. In-silico and in-vitro evaluation of human acetylcholinesterase inhibition by organophosphates. Environ. Toxicol. Pharmacol. (2018) doi:10.1016/j.etap.2017.12.014.
25. de Oliveira, N. K. S. *et al.* Molecular Docking, Physicochemical Properties, Pharmacokinetics and Toxicity of Flavonoids Present in Euterpe Oleracea Martius. Curr. Comput. Aided. Drug Des. (2020) doi:10.2174/1573409916666200619122803.
26. Wright, D. W., Hall, B. A., Kenway, O. A., Jha, S. & Coveney, P. V. Computing clinically relevant binding free energies of HIV-1 protease inhibitors. J. Chem. Theory Comput. (2014) doi:10.1021/ct4007037.
27. Kaushik, A. C., Kumar, S., Wei, D. Q. & Sahi, S. Structure Based Virtual Screening Studies to Identify Novel Potential Compounds for GPR142 and Their Relative Dynamic Analysis for Study of Type 2 Diabetes. Front. Chem. (2018) doi:10.3389/fchem.2018.00023.
28. Schrödinger Release. Desmond Molecular Dynamics System. *Schrödinger LLC* (2019).

Figures

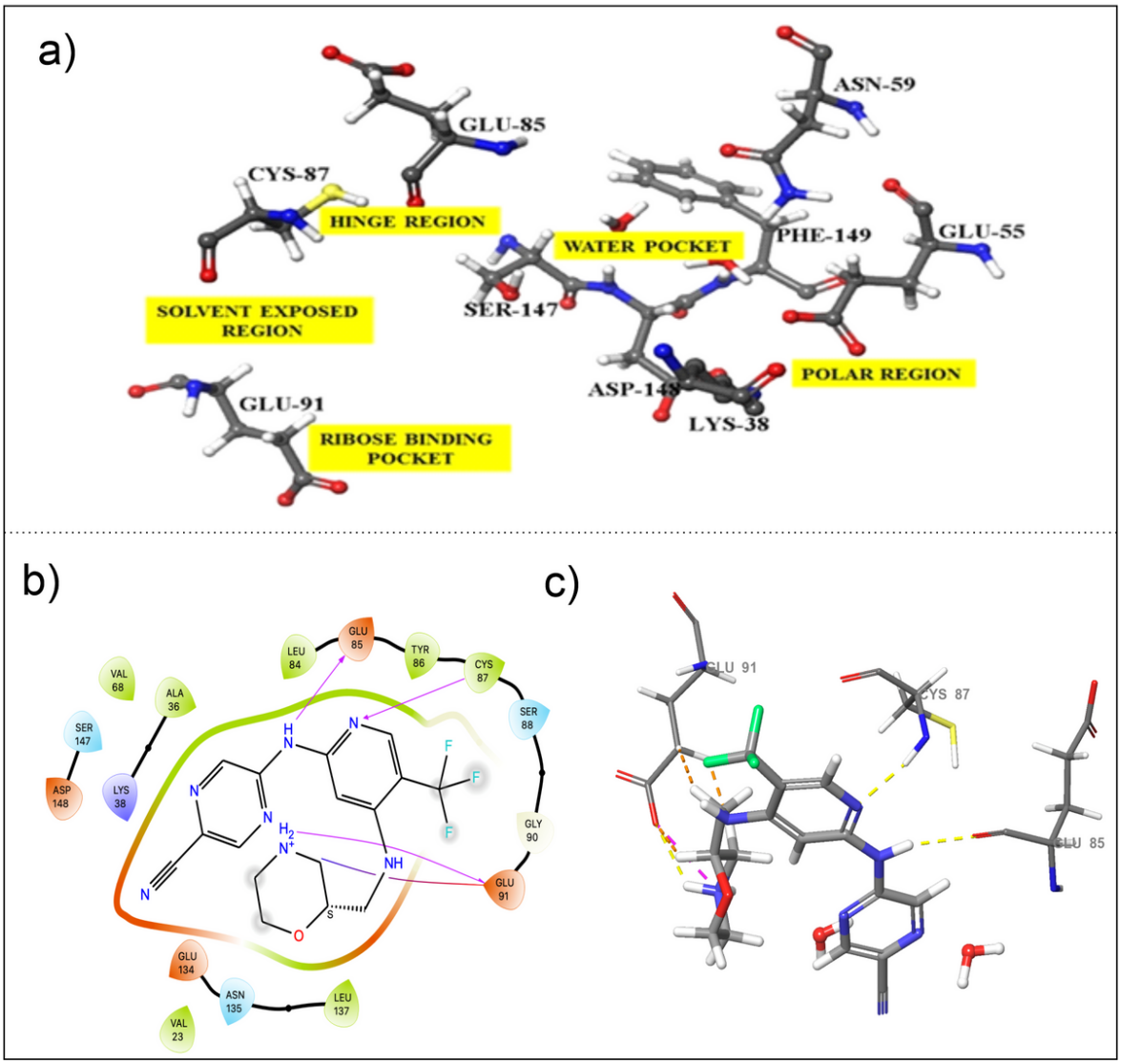

Figure 1

(a) The ATP binding site of CHK-1 depicting critical regions of amino acids that bind ligands and water molecules. Molecular docking results of co-crystallized clinical trial ligand with CHK-1 protein displaying **(b)** 2D and **(c)** 3D interaction fingerprints of ligand at ATP binding region.

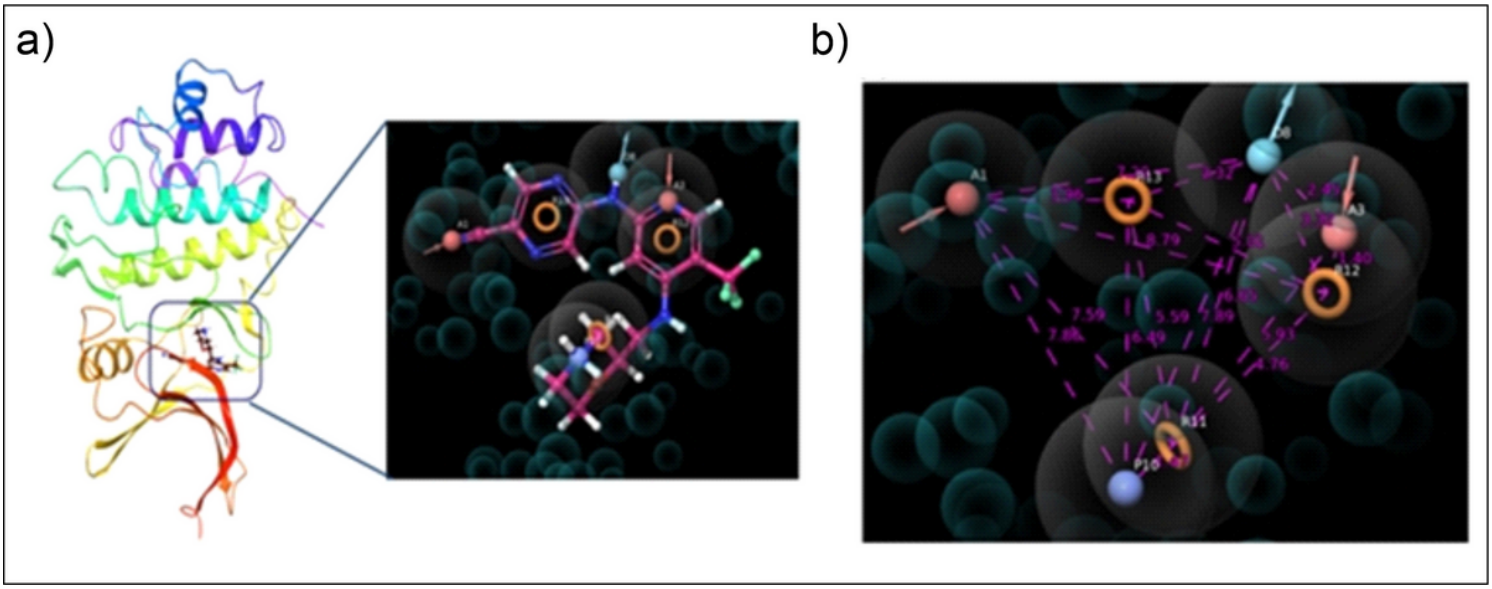

Figure 2

e-Pharmacophore features for database screening. **(a)** the seven features were selected from CCT245737 ligand. The features A1 and A3 (Pink spheres) are H-bond acceptors, D8 (Blue sphere) H-bond donor, P10 (Blue sphere) positive ionisable group and R11, R12 &R13 (Orange torus) for an aromatic ring. **(b)** Three dimensional (3D) spatial arrangement of selected features with intersite distances. The intersite distances between the selected features are represented as angstrom (Å).

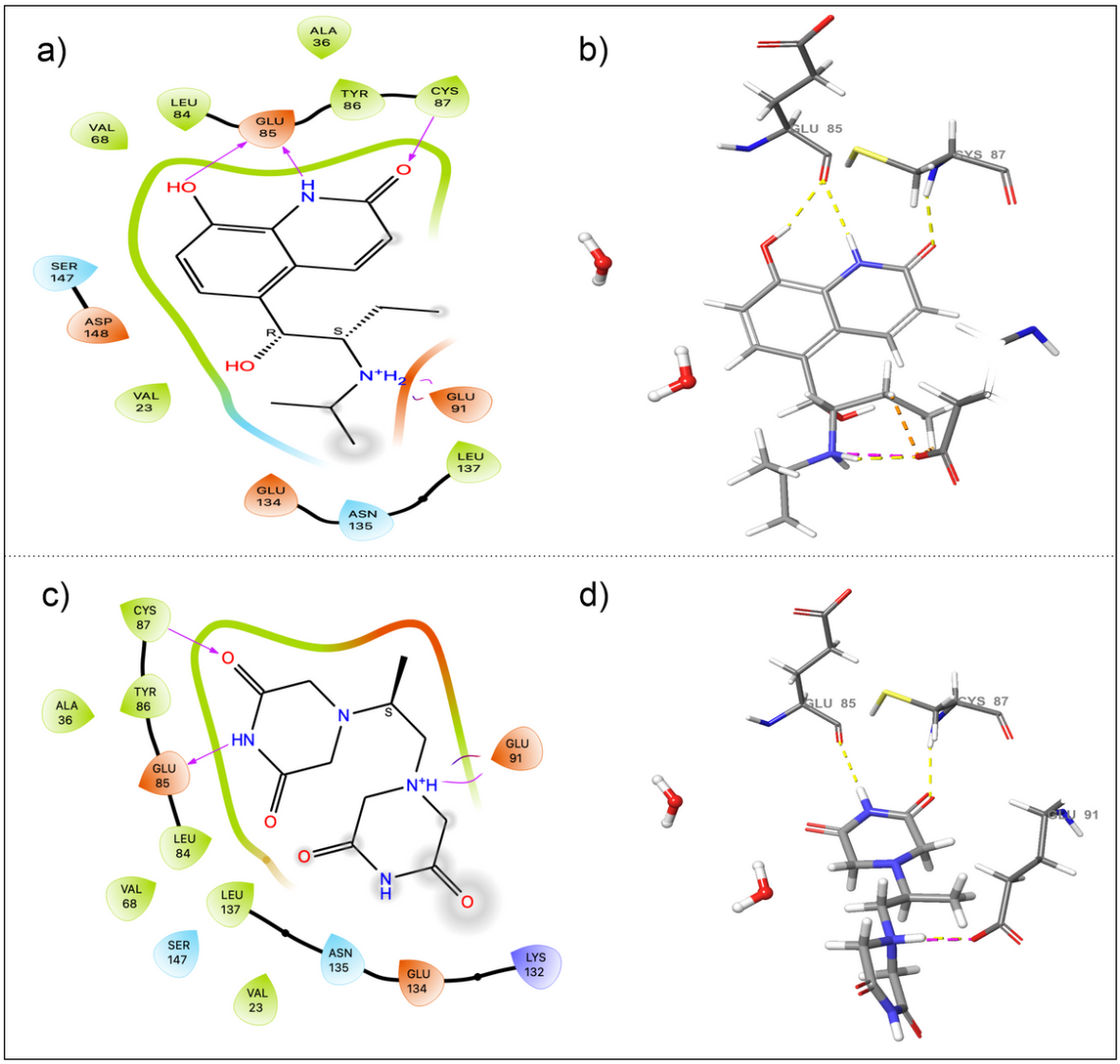

Figure 3

XP molecular docking results of CHK-1 protein with Procaterol (a & b) and Dexrazoxane (c & d). Images representing 3D interaction patterns of CHK-1 protein residues with (a) Procaterol and (c) Dexrazoxane. 2D interaction map of (b) Procaterol and (d) Dexrazoxane to the ATP binding domain.

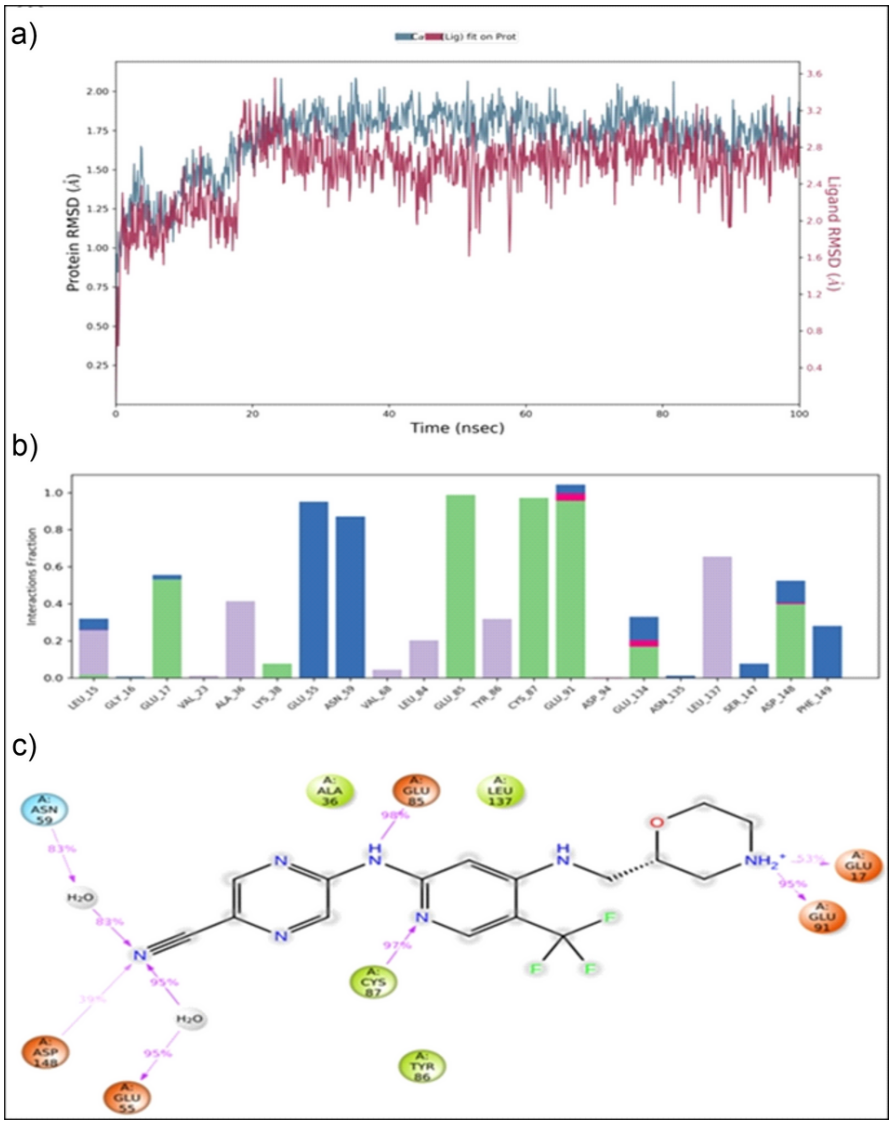

Figure 4

The MD results of clinical trial inhibitor (CCT245737)-CHK-1 complex. **(a)**MD simulation trajectories for the CCT245737 complex showing (Lig) fit on prot during 100ns simulation time, **(b)**Protein-ligand contacts between the complex and **(c)** the 2D interaction nature of CCT245737 ligand.

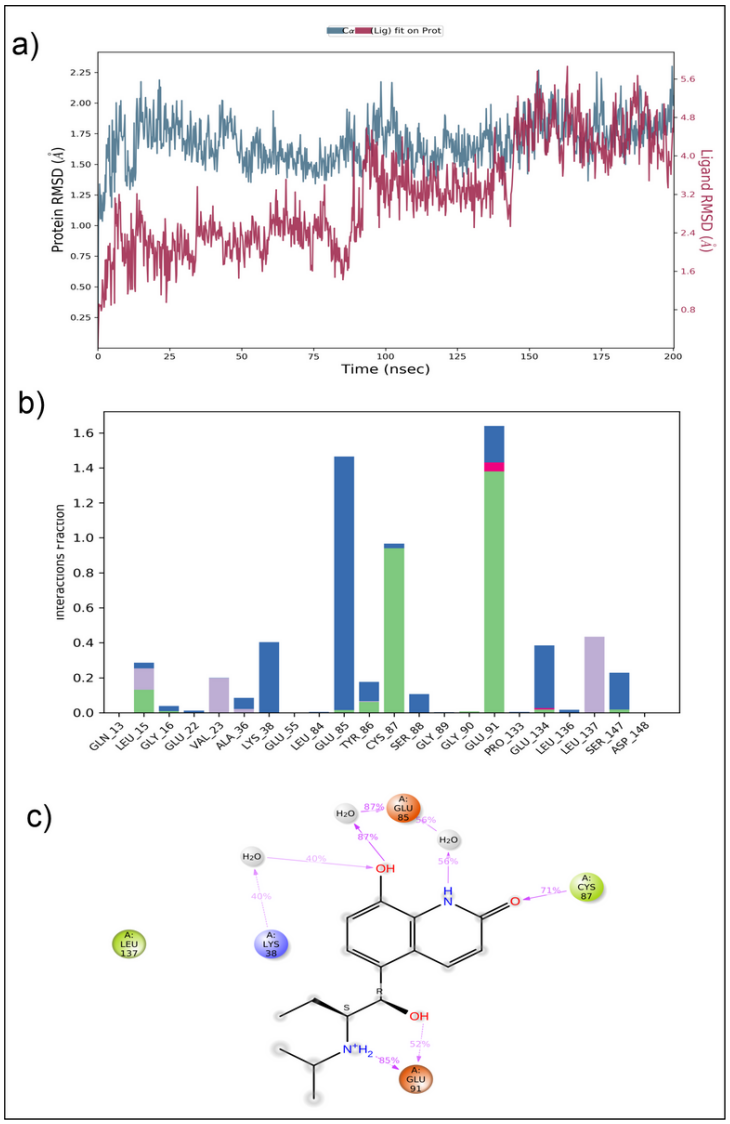

Figure 5

The MD results of Procaterol-CHK-1 complex. **(a)** the MD simulation trajectories for the Procaterol complex showing (Lig) fit on prot during 200ns simulation time. **(b)** Protein-ligand contacts between the complex. **(c)** the 2D interaction nature of Procaterol drug with ATP binding site.

Supplementary Files

This is a list of supplementary files associated with this preprint. Click to download.

- Supplementaryfiles.docx